



Synthesis, biological evaluation and molecular docking studies of 1,3,4-oxadiazole derivatives as potential immunosuppressive agents

Zhi-Ming Zhang^a, Xue-Wei Zhang^a, Zong-Zheng Zhao^a, Ru Yan^a, Rui Xu^a, Hai-Bin Gong^{b,*}, Hai-Liang Zhu^{a,*}

^a State Key Laboratory of Pharmaceutical Biotechnology, Nanjing University, Nanjing 210093, People's Republic of China

^b Xuzhou Central Hospital, Xuzhou 221009, People's Republic of China

ARTICLE INFO

Article history:

Received 7 February 2012

Revised 11 March 2012

Accepted 12 March 2012

Available online 4 April 2012

Keywords:

1,3,4-Oxadiazole derivatives
Immunosuppressive activities
PI3K γ inhibitor
Molecular docking

ABSTRACT

A series of 1,3,4-oxadiazole derivatives derived from 4-methoxysalicylic acid or 4-methylsalicylic acid (**6a–6z**) have been first synthesized for their potential immunosuppressive activity. Among them, compound **6z** displayed the most potent biological activity against lymph node cells (inhibition = 38.76% for lymph node cells and IC₅₀ = 0.31 μ M for PI3K γ). The preliminary mechanism of compound **6z** inhibition effects was also detected by flow cytometry (FCM) and the compound exerted immunosuppressive activity via inducing the apoptosis of activated lymph node cells in a dose dependent manner. Docking simulation was performed to position compound **6z** into the PI3K γ structure active site to determine the probable binding model.

© 2012 Elsevier Ltd. All rights reserved.

1. Introduction

Autoimmune diseases represent a major cause of morbidity and mortality. More than 70 autoimmune diseases have been described, and although many of these diseases are quite rare, the collective prevalence of autoimmune diseases is high. The major autoimmune diseases include psoriasis, rheumatoid arthritis, Crohn's disease, multiple sclerosis, and systemic lupus erythematosus.^{1–3} Although immunosuppressive drugs have been used for the treatment of autoimmune diseases in clinic, their side effects including liver toxicity, nephrotoxicity, infection, cardiovascular toxicity and others cannot be neglected.^{4–8} Therefore, there is a clinical need for new and less toxic therapeutic agents with new mechanisms of action.

Phosphoinositide 3-kinases (PI3Ks) are a class of enzymes that catalyze phosphorylation of the 3-hydroxyl position of phosphoinositides (PIs). The resulting second messengers, phosphatidylinositol 3,4-bisphosphate (PIP2) and phosphatidylinositol 3,4,5-trisphosphate (PIP3), can regulate a remarkably diverse array of physiological processes, including glucose homeostasis, cell growth, differentiation, and motility.^{9,10} According to their molecular structure, cellular regulation and in vivo substrate specificities, PI3Ks are divided into class I, II and III PI3Ks.^{11,12} The best known PI3Ks are class I PI3Ks, which include subclass IA (consist-

ing of PI3K α , PI3K β and PI3K δ isoforms) and subclass IB (consisting of PI3K γ isoform only). Class IA PI3Ks are activated by receptor tyrosine kinases through a p85 receptor domain, and the class IB PI3K is mainly activated by seven-transmembrane G-protein-coupled receptors (GPCRs) through its regulatory subunit p101 and G-protein $\beta\gamma$ subunits.¹¹ Because of the isoforms' differential tissue distribution, they show distinct biological functions. PI3K α and PI3K β are ubiquitously expressed and regulate functions such as cell proliferation and survival. Whereas PI3K δ and PI3K γ are mainly expressed in the hematopoietic system and mediate immune responses. It has been found that the PI3K γ isoform plays a pivotal role in inflammation and is involved in allergy, cardiovascular disorders, development of chronic inflammation, and autoimmune diseases.^{13–15} Therefore, the inhibition of PI3K γ might represent a promising therapy for autoimmune and inflammatory diseases.^{16,17}

1,3,4-Oxadiazoles are an important class of heterocyclic compounds. The widespread use of them as a scaffold in medicinal chemistry establishes this moiety as a member of the privileged structures class.¹⁸ They show broad spectrum of bioactivities.^{19–23} Among these, a few differently substituted 1,3,4-oxadiazoles have exhibited potent immunosuppressive activities particularly.^{24–26} Further, 1,3,4-oxadiazole heterocycles are very good bioisosteres of amides and esters, which can contribute substantially in increasing pharmacological activity by participating in hydrogen bonding interactions with the receptors.²⁷

As we know, salicylic acid was identified in willow bark extracts as an active anti-inflammatory compound over a century ago.

* Corresponding authors. Tel.: +86 25 8359 2572; fax: +86 25 8359 2672.

E-mail address: zhuhli@nju.edu.cn (H.-L. Zhu).

Some salicylic acid derivatives were reported to show potent anti-inflammatory activity.^{28–30} In view of the facts mentioned above, we hypothesized that 1,3,4-oxadiazole derivatives derived from 4-methoxysalicylic acid or 4-methylsalicylic acid might display potent anti-inflammatory activity. In this paper, we designed and synthesized a series of 1,3,4-oxadiazole derivatives derived from 4-methoxysalicylic acid or 4-methylsalicylic acid and studied their immunosuppressive activities and PI3K γ inhibitory activity. Biological evaluation indicated that some of the synthesized compounds were potent inhibitors of PI3K γ .

2. Results and discussion

2.1. Chemistry

In this study, 26 1,3,4-oxadiazole derivatives derived from 4-methoxysalicylic acid or 4-methylsalicylic acid were synthesized. The synthetic route of compounds **6a–6z** was shown in Scheme 1.

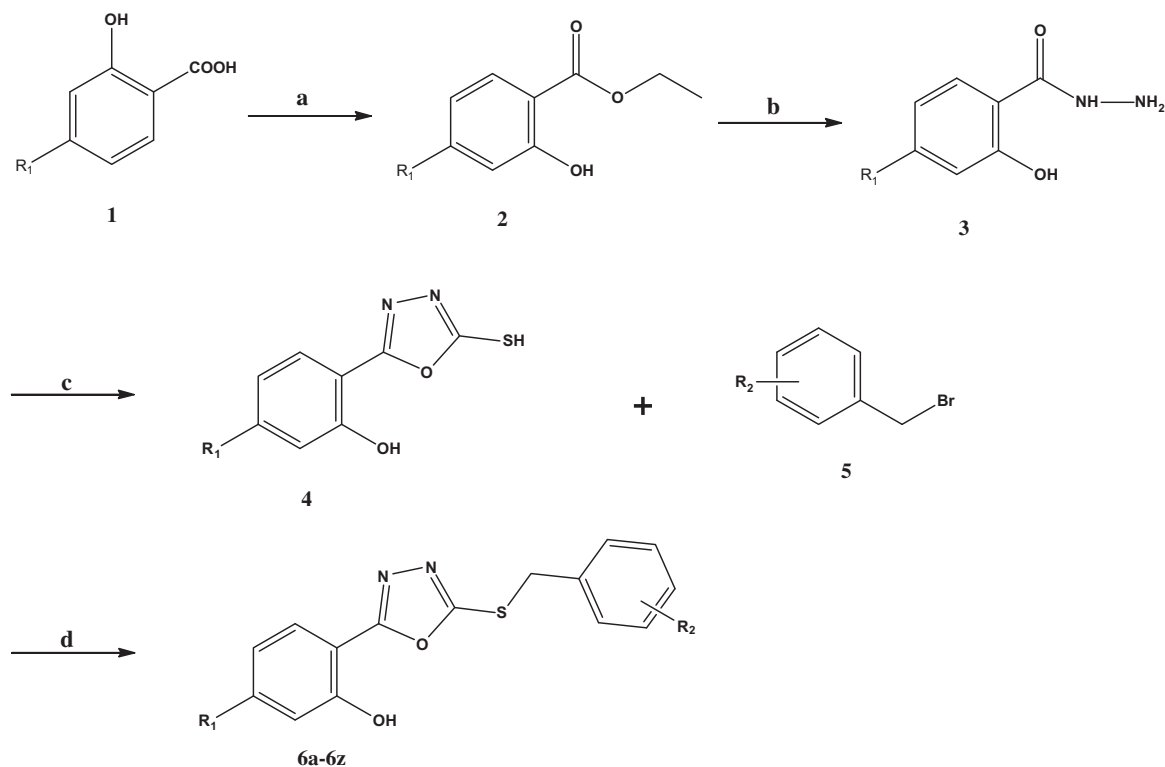
The key compound **4** was prepared in three steps. Esterification of 4-methoxysalicylic acid or 4-methylsalicylic acid **1** with ethanol

and concentrated sulfuric acid afforded the corresponding ester **2**. The aroyl hydrazide **3** was obtained by reaction of the ester **2** with 85% hydrazine monohydrate in ethanol. Treatment of the aroyl hydrazide **3** with carbon disulfide in the presence of KOH and 95% ethanol under reflux provided the key intermediate **4**. The synthesis of compounds **6a–6z** were accomplished by refluxing **4** with different substituted benzyl bromides in the presence of NaOH in acetonitrile. All target compounds were purified by recrystallisation. All of the synthetic compounds gave satisfactory analytical and spectroscopic data, which were in full accordance with their depicted structures.

2.2. Biological activity

2.2.1. Cytotoxicity test

The inhibitory activity of the compounds is sometimes a result of their toxic effects and consequently might cause an erroneous conclusion.^{31–33} Prior to the following bioactivity analysis, all the synthesized 1,3,4-oxadiazole derivatives (**6a–6z**) were tested in vitro for their cytotoxicity on lymph node cells with cyclosporin



6a	$R_1 = \text{OMe}, R_2 = \text{H}$
6b	$R_1 = \text{OMe}, R_2 = 2\text{-Cl}$
6c	$R_1 = \text{OMe}, R_2 = 3\text{-Cl}$
6d	$R_1 = \text{OMe}, R_2 = 4\text{-Cl}$
6e	$R_1 = \text{OMe}, R_2 = 2\text{-F}$
6f	$R_1 = \text{OMe}, R_2 = 4\text{-F}$
6g	$R_1 = \text{OMe}, R_2 = 3\text{-Me}$
6h	$R_1 = \text{OMe}, R_2 = 4\text{-Me}$
6i	$R_1 = \text{OMe}, R_2 = 3\text{-OMe}$
6j	$R_1 = \text{OMe}, R_2 = 4\text{-OMe}$
6k	$R_1 = \text{OMe}, R_2 = 2\text{-NO}_2$
6l	$R_1 = \text{OMe}, R_2 = 3\text{-NO}_2$
6m	$R_1 = \text{OMe}, R_2 = 4\text{-NO}_2$

6n	$R_1 = \text{Me}, R_2 = \text{H}$
6o	$R_1 = \text{Me}, R_2 = 2\text{-Cl}$
6p	$R_1 = \text{Me}, R_2 = 3\text{-Cl}$
6q	$R_1 = \text{Me}, R_2 = 4\text{-Cl}$
6r	$R_1 = \text{Me}, R_2 = 2\text{-F}$
6s	$R_1 = \text{Me}, R_2 = 4\text{-F}$
6t	$R_1 = \text{Me}, R_2 = 3\text{-Me}$
6u	$R_1 = \text{Me}, R_2 = 4\text{-Me}$
6v	$R_1 = \text{Me}, R_2 = 3\text{-OMe}$
6w	$R_1 = \text{Me}, R_2 = 4\text{-OMe}$
6x	$R_1 = \text{Me}, R_2 = 2\text{-NO}_2$
6y	$R_1 = \text{Me}, R_2 = 3\text{-NO}_2$
6z	$R_1 = \text{Me}, R_2 = 4\text{-NO}_2$

Scheme 1. General synthesis of compounds (**6a–6z**). Reagents and conditions: (a) ethanol, concentrated sulfuric acid, reflux, 8–12 h; (b) $\text{NH}_2\text{NH}_2 \cdot \text{H}_2\text{O}$ (85%), ethanol, reflux, 8–12 h; (c) (1) CS_2/KOH , ethanol (95%), reflux, 24 h, (2) HCl , pH 5–6; (d) NaOH , acetonitrile, reflux, 8–24 h.

Table 1

The cytotoxicity of the synthetic compounds (**6a–6z**) and cyclosporin A (CsA) on lymph node cells

Compound ^a	OD ₅₇₀ ^b	Compound ^a	OD ₅₇₀ ^b
6a	0.81	6n	0.86
6b	0.89	6o	0.79
6c	0.90	6p	0.70
6d	0.87	6q	0.75
6e	0.79	6r	0.82
6f	0.87	6s	0.82
6g	1.12	6t	0.80
6h	0.90	6u	0.65
6i	0.71	6v	0.87
6j	0.75	6w	0.83
6k	0.91	6x	0.74
6l	0.86	6y	0.81
6m	0.83	6z	0.89
CsA	0.51	Control	0.88

^a The compounds tested for cytotoxicity were consistent with the description in the Section 4.

^b Values are means of three experiments.

A (CsA) as the positive control. The pharmacological results were summarized in Table 1 and Figure 1. The data showed that most of the 1,3,4-oxadiazole derivatives had a quite low toxicity.

2.2.2. Inhibitory activity assay

All the synthesized 1,3,4-oxadiazole derivatives (**6a–6z**) were evaluated for their inhibitory activity on murine lymphocyte proliferation induced by Concanavalin A (ConA). The results were summarized in Table 2. Among them, compound **6z** (inhibition = 38.76%) exhibited the most potent immunosuppressive activity.

As shown in Table 2, in general, most of the 1,3,4-oxadiazole derivatives exhibited higher immunosuppressive activity than their original acids (inhibition = 7.34% for 4-methoxysalicylic acid, inhibition = 3.52% for 4-methylsalicylic acid). So the introduction of oxadiazole group was important for their immunosuppressive activity.

Structure–activity relationships in these 1,3,4-oxadiazole derivatives derived from 4-methoxysalicylic acid or 4-methylsalicylic acid demonstrated that compounds with different substituents led to different immunosuppressive activity. For compounds with halogen group on the benzene ring, compounds derived from 4-methoxysalicylic acid (**6b–6f**) showed better inhibitory activity

Table 2

Inhibitory effects of synthetic compounds (**6a–6z**) on murine lymphocyte proliferation induced by Concanavalin A (ConA)

Compound	Inhibition ^a (%)	Compound	Inhibition ^a (%)
6a	4.50	6n	9.08
6b	17.36	6o	8.99
6c	22.03	6p	−0.72
6d	11.96	6q	13.40
6e	34.35	6r	−6.92
6f	29.32	6s	4.50
6g	16.28	6t	5.22
6h	6.29	6u	11.42
6i	11.06	6v	20.59
6j	11.33	6w	13.67
6k	3.96	6x	11.42
6l	19.33	6y	−4.36
6m	14.39	6z	38.76
4-Methoxysalicylic acid	7.34	4-Methylsalicylic acid	3.52
CsA	69.77	Control	0.00

^a Values are means of three experiments.

Table 3

PI3Ks inhibitory activity of selected compounds

Compound	IC ₅₀ ^a (μM)			
	PI3Kγ	PI3Kα	PI3Kβ	PI3Kδ
6c	1.87	15.37	43.67	>100
6e	0.59	33.92	51.75	18.97
6f	0.98	31.21	>100	11.53
6l	2.47	17.94	>100	29.73
6v	2.59	1.97	13.62	>100
6z	0.31	54.93	>100	25.56
LY294002	7.26 ^b	0.50 ^c	0.97 ^c	0.57 ^c

^a Values are means of three experiments.

^b Reported value, Ref. 39.

^c Reported value, Ref. 40.

than those derived from 4-methylsalicylic acid (**6o–6s**). On the contrary, when introduced methyl, methoxy or nitro groups, compounds derived from 4-methoxysalicylic acid (**6g–6m**) displayed less potent inhibitory activity than those derived from 4-methylsalicylic acid (**6t–6z**). Furthermore, the inhibitory activity was

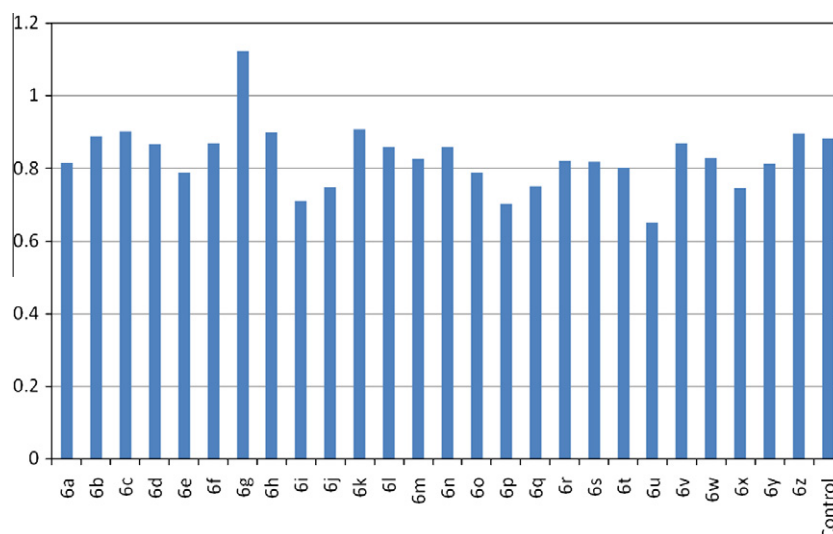


Figure 1. The cytotoxicity of the synthetic compounds (**6a–6z**) on lymph node cells. Most of the compounds exhibited nontoxic.

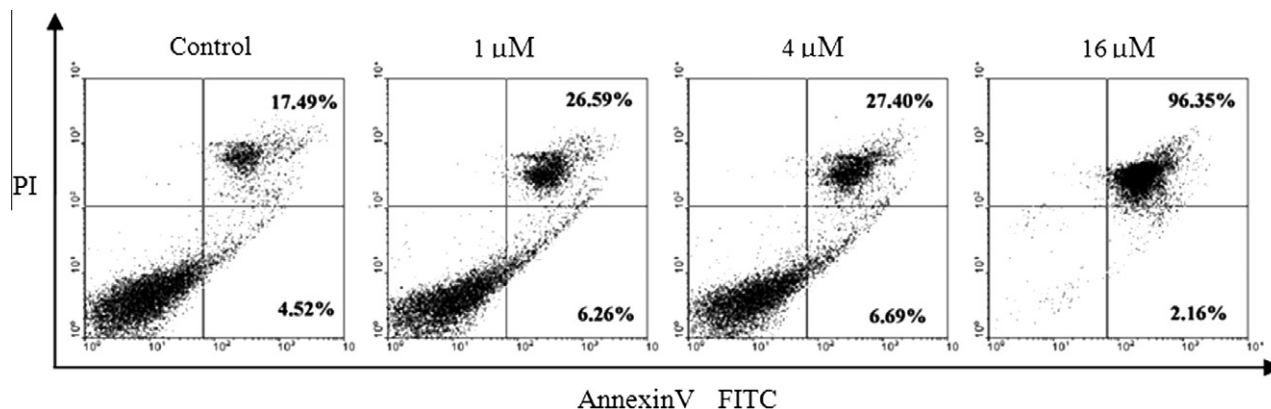


Figure 2. Lymph node cells isolated from naive mice were cultured with ConA and various concentrations of **6z** for 24 h. Cells were stained by Annexin V-FITC/PI and apoptosis was analyzed by flow cytometry. Inhibition including early and late apoptosis.

governed by the position of substituents. For compounds derived from 4-methoxysalicylic acid, the orders of the activities were as follows: chloro group at the *meta* position (**6c**) > chloro group at the *ortho* position (**6b**) > chloro group at the *para* position (**6d**), fluoro group at the *ortho* position (**6e**) > fluoro group at the *para* position (**6f**), methyl group at the *meta* position (**6g**) > methyl group at the *para* position (**6h**) and methoxy group at the *para* position (**6j**) > methoxy group at the *meta* position (**6i**). However, the potency orders changed when these substituents were introduced to 1,3,4-oxadiazole derivatives derived from 4-methylsalicylic acid (**6o–6w**). Compound **6z** with nitro group at the *para* position on the benzene ring showed the most potent activity of all compounds, interestingly, introduction of nitro group to the *meta* position, afforded **6y** with a remarkable decrease in the immunosuppressive activity. From the results of molecular docking studies of compound **6z**, we could find that nitro group at the *para* position could form a hydrogen bond with LYS890, which was helpful for the inhibitory activity of compound **6z**.

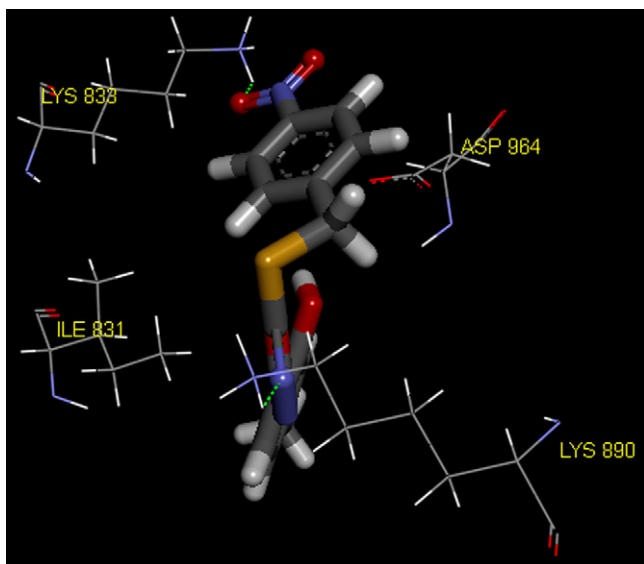


Figure 3. Molecular docking modeling of compound **6z** with PI3K γ : compound **6z** was nicely bound to PI3K γ with its nitrogen atom of oxadiazole group forming a hydrogen bond with the amino hydrogen of LYS890 (H–N...H: 2.048 Å, 123.251°), and the oxygen atom of the nitro group of **6z** also formed a hydrogen bond with the hydrogen atom of LYS833 (H–O...H: 1.766 Å, 127.672°).

2.2.3. PI3Ks inhibitory assay

Selected compounds (**6c**, **6e**, **6f**, **6l**, **6v**, **6z**) that exhibited significant immunosuppressive activities were evaluated for their PI3Ks inhibitory activity with LY294002, a well-known class I PI3K inhibitor, as the positive control.^{34,35} The results were presented in Table 3. Most of the selected compounds displayed good inhibitory activity on PI3K γ and selectivity over PI3K α , PI3K β and PI3K δ . Among them, compound **6z** showed the most potent PI3K γ inhibitory activity with IC₅₀ of 0.31 μM. The results of PI3K γ inhibitory activity of the tested compounds were corresponding to the structure–activity relationships (SAR) of their immunosuppressive activities. And the binding model of compound **6z** into ATP binding site of PI3K γ also demonstrated that the potent immunosuppressive activities of the synthetic compounds were probably correlated to their PI3K γ inhibitory activities.

2.2.4. Apoptosis assay

Apoptosis is an essential mechanism used to eliminate activated T cells during the shutdown process of excess immune responses and maintains proper immune homeostasis, while deficient apoptosis of activated T cells is associated with a wide variety of immune disorders. As representative of these 1,3,4-oxadiazole derivatives, compounds **6z** was studied in vitro. We detected the mechanism of compound **6z** inhibition effect by flow cytometry (FCM) (Fig. 2), and found that the compound could induce the apoptosis of activated lymph node cells in a dose dependent manner. As shown in Figure 2, lymph node cells stimulated with ConA were treated with 0, 1, 4 and 16 μM of compound **6z** for 24 h. The compound increased the percentage of apoptosis by Annexin V-FITC/PI staining in a dose-dependent manner. And the cytotoxicity test displayed that compound **6z** showed quite low toxicity at the concentration of 16 μM (OD₅₇₀ = 0.85). These results above indicated that compound **6z** could induce apoptosis of ConA stimulated lymph node cells.

2.3. Binding model of compounds **6v** and **6z** into PI3K γ structure

In an effort to elucidate the mechanism by which the title compounds could induce immunosuppressive activity against T cells and guide further SAR studies, molecular modeling of the potent inhibitor **6z** into ATP binding site of PI3K γ was performed to simulate a binding model based on PI3K γ structure (3L54.pdb). The binding model of compound **6z** and PI3K γ were depicted in Figures 3 and 4. In the binding model, compound **6z** was nicely bound to PI3K γ

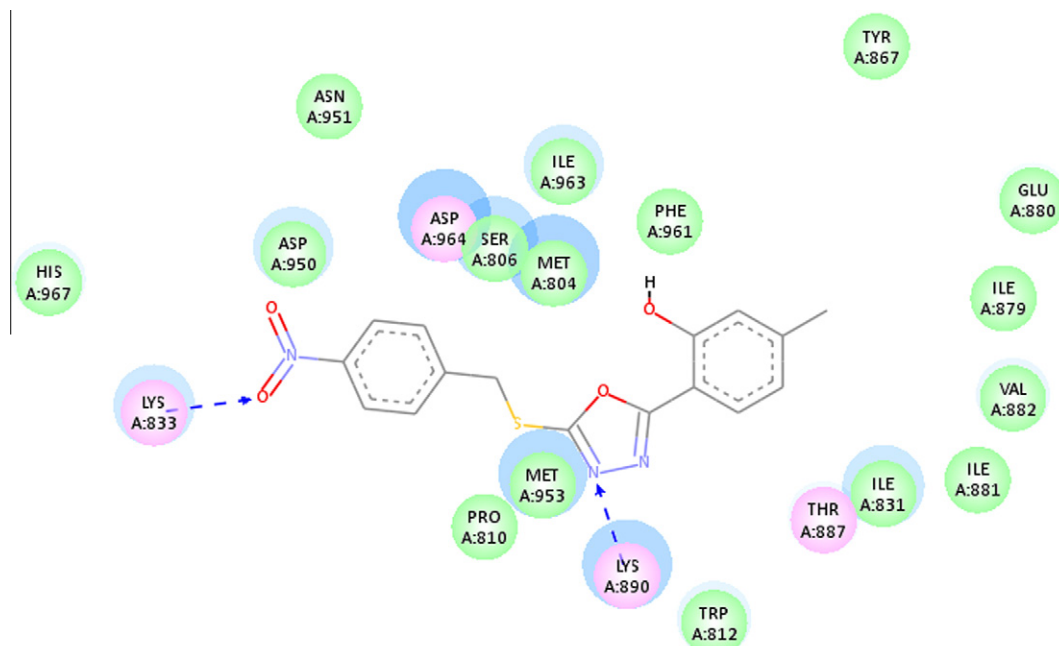


Figure 4. 2D ligand interaction diagram of compound **6z** with PI3K γ with the essential amino acid residues at the binding site tagged in circles. The purple circles showed the amino acids which participated in hydrogen bonding, electrostatic or polar interactions and the green circles showed the amino acids which participated in the Van der Waals interactions. Two hydrogen bond interactions between compound **6z** and PI3K γ were indicated.

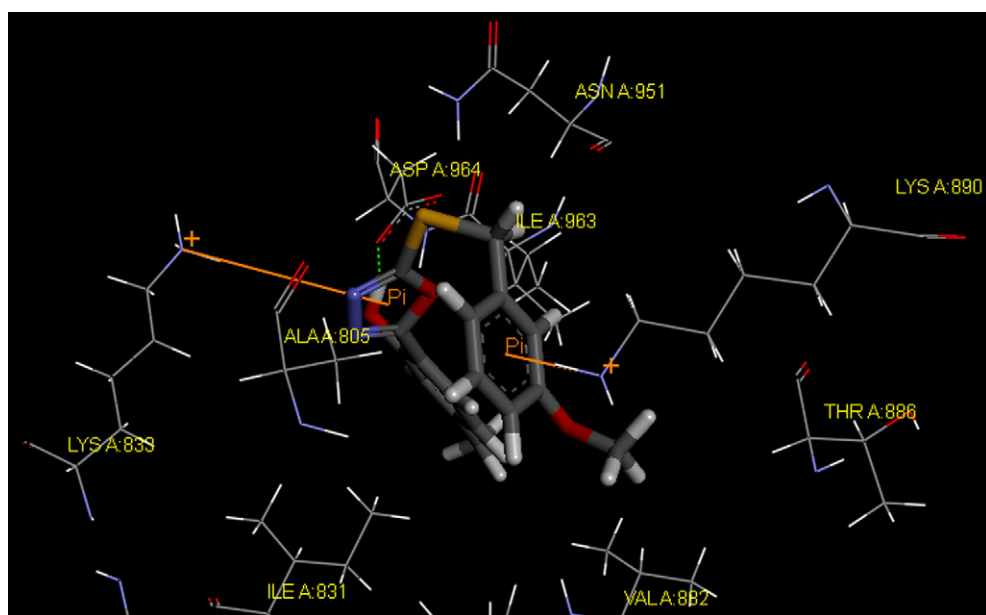


Figure 5. Molecular docking modeling of compound **6v** with PI3K γ : compound **6v** was bond to PI3K γ with its hydroxyl of 4-methylsalicylic acid group forming a hydrogen bond with the oxygen atom of ASP964 (H–O...H: 1.091 Å, 161.935°). Meanwhile, two π -cation interactions were also formed.

with its nitrogen atom of oxadiazole group forming a hydrogen bond with the amino hydrogen of LYS890 (H–N...H: 2.048 Å, 123.251°), and the oxygen atom of the nitro group of **6z** also formed a hydrogen bond with the hydrogen atom of LYS833 (H–O...H: 1.766 Å, 127.672°). For a comparison, the binding model of the less potent compound **6v** with PI3K γ was also performed. As shown in Figures 5 and 6, compound **6v** was bond to PI3K γ with its hydroxyl

of 4-methylsalicylic acid group forming a hydrogen bond with the oxygen atom of ASP964 (H–O...H: 1.091 Å, 161.935°). Meanwhile, two π -cation interactions were also formed. So the hydrogen bond formed by oxadiazole group was important for immunosuppressive activity and the nitro group took a great role in the binding. The molecular docking results suggested that compound **6z** was a potential inhibitor of PI3K γ .

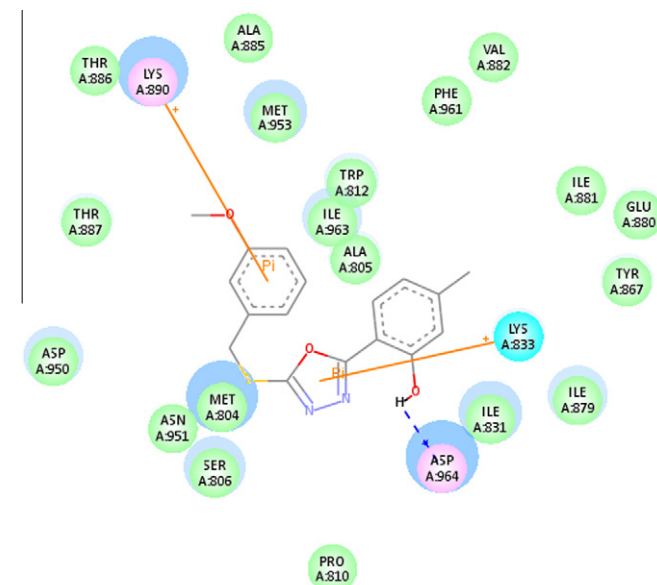


Figure 6. 2D ligand interaction diagram of compound **6v** with PI3K γ with the essential amino acid residues at the binding site tagged in circles. The purple circles showed the amino acids which participated in hydrogen bonding, electrostatic or polar interactions and the green circles showed the amino acids which participated in the Van der Waals interactions. A hydrogen bond interaction and two π -cation interactions between compound **6v** and PI3K γ were indicated.

3. Conclusions

In summary, a series of 1,3,4-oxadiazole derivatives derived from 4-methoxysalicylic acid or 4-methylsalicylic acid have been synthesized and their immunosuppressive activities against ConA stimulated T cells proliferation were evaluated. Preliminary results showed that most of the compounds displayed enhanced inhibitory activities and low toxicity. Compound **6z** demonstrated the most potent inhibitory activity that inhibited the ConA stimulated T cells with inhibition of 38.76% and inhibited the activity of PI3K γ with IC₅₀ of 0.31 μ M. Moreover, the preliminary mechanism of compound **6z** inhibition effects was also detected by flow cytometry (FCM), and the compound exerted immunosuppressive activity via inducing the apoptosis of activated lymph node cells in a dose dependent manner. Molecular docking study indicated that compound **6z** was nicely bound to the PI3K γ with two hydrogen bonds. All the results showed the great potential of compound **6z** as an immunosuppressant targeting PI3K γ .

4. Experimental section

4.1. Chemistry general

All chemicals and reagents used in current study were of analytical grade purchased from Aldrich (USA). The reactions were monitored by thin layer chromatography (TLC) on Merck pre-coated silica GF254 plates. Melting points (uncorrected) were determined on a XT4MP apparatus (Tai ke Corp., Beijing, China). ESI mass spectra were obtained on a Mariner System 5304 mass spectrometer, and ¹H NMR spectra were recorded on a DPX500 spectrometer at 25 °C with TMS and solvent signals allotted as internal standards. Chemical shifts are reported in ppm (δ). Elemental analyses were performed on a CHN-O-Rapid instrument and were within $\pm 0.4\%$ of the theoretical values.

4.2. General procedure for synthesis of the target compounds (6a–6z)

To a stirred solution of 2-(5-mercapto-1,3,4-oxadiazol-2-yl)-5-methoxyphenol (1 mmol, 0.224 g) or 2-(5-mercapto-1,3,4-oxadiazol-2-yl)-5-methylphenol (1 mmol, 0.208 g) and sodium hydroxide (1 mmol, 0.04 g) in acetonitrile (50 mL) was added corresponding benzyl bromides (1 mmol). The resulting mixture was heated under reflux for 24 h and the reaction was monitored by thin layer chromatography (TLC). Afterwards the solution was cooled to room temperature and the organic solvent was removed in vacuo. The residue was dissolved in ethyl acetate and the organic layer was washed with water and saturated brine. Then the organic phase was dried over anhydrous Na₂SO₄, filtered, and removed in vacuo. The purification of the residue by recrystallization from acetonitrile yielded the desired compounds **6a–6z**.

4.2.1. 2-(5-(Benzylthio)-1,3,4-oxadiazol-2-yl)-5-methoxyphenol (6a)

White crystal, yield 79%, mp: 110–111 °C. ¹H NMR (300 MHz, *d*₆-DMSO) δ : 3.80 (s, 3H), 4.55 (s, 2H), 6.59–6.63 (m, 2H), 7.26–7.37 (m, 3H), 7.46–7.49 (m, 2H), 7.64–7.67 (m, 1H), 10.24 (s, 1H). MS (ESI): 315.07 (C₁₆H₁₅N₂O₃S, [M+H]⁺). Anal. Calcd for C₁₆H₁₄N₂O₃S: C, 61.13; H, 4.49; N, 8.91; Found: C, 61.18; H, 4.50; N, 8.84.

4.2.2. 2-(5-((2-Chlorobenzyl)thio)-1,3,4-oxadiazol-2-yl)-5-methoxyphenol (6b)

White crystal, yield 70%, mp: 103–104 °C. ¹H NMR (300 MHz, *d*₆-DMSO) δ : 3.80 (s, 3H), 4.62 (s, 2H), 6.60–6.63 (m, 2H), 7.32–7.39 (m, 2H), 7.50–7.52 (m, 1H), 7.60–7.67 (m, 2H), 10.26 (s, 1H). MS (ESI): 349.03 (C₁₆H₁₄ClN₂O₃S, [M+H]⁺). Anal. Calcd for C₁₆H₁₃ClN₂O₃S: C, 55.09; H, 3.76; N, 8.03; Found: C, 55.16; H, 3.78; N, 8.01.

4.2.3. 2-(5-((3-Chlorobenzyl)thio)-1,3,4-oxadiazol-2-yl)-5-methoxyphenol (6c)

White crystal, yield 76%, mp: 115–116 °C. ¹H NMR (300 MHz, *d*₆-DMSO) δ : 3.80 (s, 3H), 4.55 (s, 2H), 6.59–6.63 (m, 2H), 7.34–7.40 (m, 1H), 7.43–7.47 (m, 1H), 7.57 (s, 2H), 7.64–7.67 (m, 1H), 10.25 (s, 1H). MS (ESI): 349.03 (C₁₆H₁₄ClN₂O₃S, [M+H]⁺). Anal. Calcd for C₁₆H₁₃ClN₂O₃S: C, 55.09; H, 3.76; N, 8.03; Found: C, 55.17; H, 3.78; N, 8.00.

4.2.4. 2-(5-((4-Chlorobenzyl)thio)-1,3,4-oxadiazol-2-yl)-5-methoxyphenol (6d)

White powder, yield 72%, mp: 105–106 °C. ¹H NMR (300 MHz, *d*₆-DMSO) δ : 3.80 (s, 3H), 4.54 (s, 2H), 6.58–6.63 (m, 2H), 7.34–7.43 (m, 2H), 7.49–7.52 (m, 2H), 7.64–7.67 (m, 1H), 10.24 (s, 1H). MS (ESI): 349.03 (C₁₆H₁₄ClN₂O₃S, [M+H]⁺). Anal. Calcd for C₁₆H₁₃ClN₂O₃S: C, 55.09; H, 3.76; N, 8.03; Found: C, 55.12; H, 3.77; N, 8.00.

4.2.5. 2-(5-((2-Fluorobenzyl)thio)-1,3,4-oxadiazol-2-yl)-5-methoxyphenol (6e)

White crystal, yield 71%, mp: 104–105 °C. ¹H NMR (300 MHz, *d*₆-DMSO) δ : 3.80 (s, 3H), 4.57 (s, 2H), 6.60–6.63 (m, 2H), 7.15–7.25 (m, 2H), 7.33–7.40 (m, 1H), 7.52–7.58 (m, 1H), 7.64–7.67 (m, 1H), 10.24 (s, 1H). MS (ESI): 333.06 (C₁₆H₁₄FN₂O₃S, [M+H]⁺). Anal. Calcd for C₁₆H₁₃FN₂O₃S: C, 57.82; H, 3.94; N, 8.43; Found: C, 57.84; H, 3.96; N, 8.40.

4.2.6. 2-(5-((4-Fluorobenzyl)thio)-1,3,4-oxadiazol-2-yl)-5-methoxyphenol (6f)

White crystal, yield 74%, mp: 110–111 °C. ¹H NMR (300 MHz, *d*₆-DMSO) δ : 3.80 (s, 3H), 4.55 (s, 2H), 6.59–6.63 (m, 2H), 7.14–7.20

(m, 2H), 7.50–7.55 (m, 2H), 7.64–7.67 (m, 1H), 10.25 (s, 1H). MS (ESI): 333.06 ($C_{16}H_{14}FN_2O_3S$, $[M+H]^+$). Anal. Calcd for $C_{16}H_{13}FN_2O_3S$: C, 57.82; H, 3.94; N, 8.43; Found: C, 57.87; H, 3.92; N, 8.44.

4.2.7. 5-Methoxy-2-(5-((3-methylbenzyl)thio)-1,3,4-oxadiazol-2-yl)phenol (6g)

White crystal, yield 64%, mp: 99–100 °C. 1H NMR (300 MHz, d_6 -DMSO) δ : 2.28 (s, 3H), 3.80 (s, 3H), 4.51 (s, 2H), 6.60–6.62 (m, 2H), 7.10 (d, J = 7.0 Hz, 1H), 7.20–7.28 (m, 3H), 7.64–7.67 (m, 1H), 10.24 (s, 1H). MS (ESI): 329.09 ($C_{17}H_{17}N_2O_3S$, $[M+H]^+$). Anal. Calcd for $C_{17}H_{16}N_2O_3S$: C, 62.18; H, 4.91; N, 8.53; Found: C, 62.22; H, 4.90; N, 8.52.

4.2.8. 5-Methoxy-2-(5-((4-methylbenzyl)thio)-1,3,4-oxadiazol-2-yl)phenol (6h)

White crystal, yield 68%, mp: 129–130 °C. 1H NMR (300 MHz, d_6 -DMSO) δ : 2.27 (s, 3H), 3.80 (s, 3H), 4.51 (s, 2H), 6.60–6.63 (m, 2H), 7.14 (d, J = 8.0 Hz, 2H), 7.35 (d, J = 8.0 Hz, 2H), 7.64–7.68 (m, 1H), 10.24 (s, 1H). MS (ESI): 329.09 ($C_{17}H_{17}N_2O_3S$, $[M+H]^+$). Anal. Calcd for $C_{17}H_{16}N_2O_3S$: C, 62.18; H, 4.91; N, 8.53; Found: C, 62.26; H, 4.93; N, 8.50.

4.2.9. 5-Methoxy-2-(5-((3-methoxybenzyl)thio)-1,3,4-oxadiazol-2-yl)phenol (6i)

White crystal, yield 60%, mp: 97–98 °C. 1H NMR (300 MHz, d_6 -DMSO) δ : 3.72 (s, 3H), 3.80 (s, 3H), 4.52 (s, 2H), 6.59–6.62 (m, 2H), 6.84–6.87 (m, 1H), 7.02–7.05 (m, 2H), 7.26 (t, J = 8.2 Hz, 1H), 7.65–7.68 (m, 1H), 10.25 (s, 1H). MS (ESI): 345.08 ($C_{17}H_{17}N_2O_4S$, $[M+H]^+$). Anal. Calcd for $C_{17}H_{16}N_2O_4S$: C, 59.29; H, 4.68; N, 8.13; Found: C, 59.34; H, 4.71; N, 8.10.

4.2.10. 5-Methoxy-2-(5-((4-methoxybenzyl)thio)-1,3,4-oxadiazol-2-yl)phenol (6j)

White crystal, yield 63%, mp: 112–113 °C. 1H NMR (300 MHz, d_6 -DMSO) δ : 3.73 (s, 3H), 3.80 (s, 3H), 4.50 (s, 2H), 6.59–6.63 (m, 2H), 6.89 (d, J = 8.6 Hz, 2H), 7.39 (d, J = 8.6 Hz, 2H), 7.65–7.68 (m, 1H), 10.25 (s, 1H). MS (ESI): 345.08 ($C_{17}H_{17}N_2O_4S$, $[M+H]^+$). Anal. Calcd for $C_{17}H_{16}N_2O_4S$: C, 59.29; H, 4.68; N, 8.13; Found: C, 59.36; H, 4.71; N, 8.09.

4.2.11. 5-Methoxy-2-(5-((2-nitrobenzyl)thio)-1,3,4-oxadiazol-2-yl)phenol (6k)

Light yellow crystal, yield 60%, mp: 127–128 °C. 1H NMR (300 MHz, d_6 -DMSO) δ : 3.80 (s, 3H), 4.81 (s, 2H), 6.60–6.63 (m, 2H), 7.58–7.66 (m, 2H), 7.73–7.81 (m, 2H), 8.12 (d, J = 8.0 Hz, 1H), 10.26 (s, 1H). MS (ESI): 360.06 ($C_{16}H_{14}N_3O_5S$, $[M+H]^+$). Anal. Calcd for $C_{16}H_{13}N_3O_5S$: C, 53.48; H, 3.65; N, 11.69; Found: C, 53.53; H, 3.66; N, 11.66.

4.2.12. 5-Methoxy-2-(5-((3-nitrobenzyl)thio)-1,3,4-oxadiazol-2-yl)phenol (6l)

Brown crystal, yield 65%, mp: 132–133 °C. 1H NMR (300 MHz, d_6 -DMSO) δ : 3.80 (s, 3H), 4.69 (s, 2H), 6.57–6.60 (m, 2H), 7.63–7.68 (m, 2H), 7.96 (d, J = 7.9 Hz, 1H), 8.14–8.17 (m, 1H), 8.40 (t, J = 2.0 Hz, 1H), 10.24 (s, 1H). MS (ESI): 360.06 ($C_{16}H_{14}N_3O_5S$, $[M+H]^+$). Anal. Calcd for $C_{16}H_{13}N_3O_5S$: C, 53.48; H, 3.65; N, 11.69; Found: C, 53.52; H, 3.63; N, 11.68.

4.2.13. 5-Methoxy-2-(5-((4-nitrobenzyl)thio)-1,3,4-oxadiazol-2-yl)phenol (6m)

Yellow crystal, yield 67%, mp: 166–167 °C. 1H NMR (300 MHz, d_6 -DMSO) δ : 3.79 (s, 3H), 4.67 (s, 2H), 6.58–6.62 (m, 2H), 7.63–7.66 (m, 1H), 7.77 (d, J = 8.8 Hz, 2H), 8.21 (d, J = 8.8 Hz, 2H), 10.24 (s, 1H). MS (ESI): 360.06 ($C_{16}H_{14}N_3O_5S$, $[M+H]^+$). Anal. Calcd for $C_{16}H_{13}N_3O_5S$: C, 53.48; H, 3.65; N, 11.69; Found: C, 53.54; H, 3.63; N, 11.65.

4.2.14. 2-(5-(Benzylthio)-1,3,4-oxadiazol-2-yl)-5-methylphenol (6n)

White crystal, yield 77%, mp: 103–104 °C. 1H NMR (300 MHz, d_6 -DMSO) δ : 2.31 (s, 3H), 4.56 (s, 2H), 6.83 (d, J = 8.0 Hz, 1H), 6.88 (s, 1H), 7.26–7.37 (m, 3H), 7.48 (d, J = 6.8 Hz, 2H), 7.61 (d, J = 8.0 Hz, 1H), 10.09 (s, 1H). MS (ESI): 299.08 ($C_{16}H_{15}N_2O_2S$, $[M+H]^+$). Anal. Calcd for $C_{16}H_{14}N_2O_2S$: C, 64.41; H, 4.73; N, 9.39; Found: C, 64.45; H, 4.74; N, 9.35.

4.2.15. 2-(5-((2-Chlorobenzyl)thio)-1,3,4-oxadiazol-2-yl)-5-methylphenol (6o)

White powder, yield 79%, mp: 148–149 °C. 1H NMR (300 MHz, d_6 -DMSO) δ : 2.31 (s, 3H), 4.63 (s, 2H), 6.83 (d, J = 8.0 Hz, 1H), 6.89 (s, 1H), 7.31–7.39 (m, 2H), 7.49–7.52 (m, 1H), 7.60–7.64 (m, 2H), 10.11 (s, 1H). MS (ESI): 333.04 ($C_{16}H_{14}ClN_2O_2S$, $[M+H]^+$). Anal. Calcd for $C_{16}H_{13}ClN_2O_2S$: C, 57.74; H, 3.94; N, 8.42; Found: C, 57.78; H, 3.96; N, 8.36.

4.2.16. 2-(5-((3-Chlorobenzyl)thio)-1,3,4-oxadiazol-2-yl)-5-methylphenol (6p)

White crystal, yield 77%, mp: 130–131 °C. 1H NMR (300 MHz, d_6 -DMSO) δ : 2.31 (s, 3H), 4.56 (s, 2H), 6.83 (d, J = 7.7 Hz, 1H), 6.89 (s, 1H), 7.36–7.41 (m, 2H), 7.45–7.47 (m, 1H), 7.58–7.62 (m, 2H), 10.09 (s, 1H). MS (ESI): 333.04 ($C_{16}H_{14}ClN_2O_2S$, $[M+H]^+$). Anal. Calcd for $C_{16}H_{13}ClN_2O_2S$: C, 57.74; H, 3.94; N, 8.42; Found: C, 57.79; H, 3.96; N, 8.40.

4.2.17. 2-(5-((4-Chlorobenzyl)thio)-1,3,4-oxadiazol-2-yl)-5-methylphenol (6q)

White crystal, yield 80%, mp: 142–143 °C. 1H NMR (300 MHz, d_6 -DMSO) δ : 2.31 (s, 3H), 4.55 (s, 2H), 6.83 (d, J = 7.9 Hz, 1H), 6.88 (s, 1H), 7.39–7.42 (m, 2H), 7.50–7.53 (m, 2H), 7.61 (d, J = 7.9 Hz, 1H), 10.10 (s, 1H). MS (ESI): 333.04 ($C_{16}H_{14}ClN_2O_2S$, $[M+H]^+$). Anal. Calcd for $C_{16}H_{13}ClN_2O_2S$: C, 57.74; H, 3.94; N, 8.42; Found: C, 57.78; H, 3.93; N, 8.39.

4.2.18. 2-(5-((2-Fluorobenzyl)thio)-1,3,4-oxadiazol-2-yl)-5-methylphenol (6r)

White crystal, yield 74%, mp: 118–119 °C. 1H NMR (300 MHz, d_6 -DMSO) δ : 2.31 (s, 3H), 4.58 (s, 2H), 6.83 (d, J = 8.1 Hz, 1H), 6.89 (s, 1H), 7.15–7.26 (m, 2H), 7.33–7.41 (m, 1H), 7.53–7.59 (m, 1H), 7.61 (d, J = 8.0 Hz, 1H), 10.09 (s, 1H). MS (ESI): 317.07 ($C_{16}H_{14}FN_2O_2S$, $[M+H]^+$). Anal. Calcd for $C_{16}H_{13}FN_2O_2S$: C, 60.75; H, 4.14; N, 8.86; Found: C, 60.79; H, 4.15; N, 8.82.

4.2.19. 2-(5-((4-Fluorobenzyl)thio)-1,3,4-oxadiazol-2-yl)-5-methylphenol (6s)

White crystal, yield 75%, mp: 125–126 °C. 1H NMR (300 MHz, d_6 -DMSO) δ : 2.31 (s, 3H), 4.55 (s, 2H), 6.83 (d, J = 7.9 Hz, 1H), 6.88 (s, 1H), 7.14–7.21 (m, 2H), 7.51–7.55 (m, 2H), 7.61 (d, J = 7.9 Hz, 1H), 10.10 (s, 1H). MS (ESI): 317.07 ($C_{16}H_{14}FN_2O_2S$, $[M+H]^+$). Anal. Calcd for $C_{16}H_{13}FN_2O_2S$: C, 60.75; H, 4.14; N, 8.86; Found: C, 60.79; H, 4.16; N, 8.81.

4.2.20. 5-Methyl-2-(5-((3-methylbenzyl)thio)-1,3,4-oxadiazol-2-yl)phenol (6t)

White crystal, yield 72%, mp: 115–116 °C. 1H NMR (300 MHz, d_6 -DMSO) δ : 2.28 (s, 3H), 2.31 (s, 3H), 4.52 (s, 2H), 6.83 (d, J = 8.0 Hz, 1H), 6.89 (s, 1H), 7.10 (d, J = 6.8 Hz, 1H), 7.20–7.29 (m, 3H), 7.61 (d, J = 7.9 Hz, 1H), 10.09 (s, 1H). MS (ESI): 313.09 ($C_{17}H_{17}N_2O_2S$, $[M+H]^+$). Anal. Calcd for $C_{17}H_{16}N_2O_2S$: C, 65.36; H, 5.16; N, 8.97; Found: C, 65.41; H, 5.18; N, 8.94.

4.2.21. 5-Methyl-2-(5-((4-methylbenzyl)thio)-1,3,4-oxadiazol-2-yl)phenol (**6u**)

White crystal, yield 62%, mp: 166–167 °C. ¹H NMR (300 MHz, *d*₆-DMSO) δ: 2.27 (s, 3H), 2.31 (s, 3H), 4.52 (s, 2H), 6.83 (d, *J* = 8.0 Hz, 1H), 6.89 (s, 1H), 7.14 (d, *J* = 8.0 Hz, 2H), 7.36 (d, *J* = 8.0 Hz, 2H), 7.62 (d, *J* = 7.9 Hz, 1H), 10.09 (s, 1H). MS (ESI): 313.09 (C₁₇H₁₇N₂O₂S, [M+H]⁺). Anal. Calcd for C₁₇H₁₆N₂O₂S: C, 65.36; H, 5.16; N, 8.97; Found: C, 65.40; H, 5.15; N, 8.95.

4.2.22. 2-(5-((3-Methoxybenzyl)thio)-1,3,4-oxadiazol-2-yl)-5-methylphenol (**6v**)

White crystal, yield 63%, mp: 111–112 °C. ¹H NMR (300 MHz, *d*₆-DMSO) δ: 2.31 (s, 3H), 3.72 (s, 3H), 4.53 (s, 2H), 6.81–6.89 (m, 3H), 7.03–7.05 (m, 2H), 7.26 (t, *J* = 8.2 Hz, 1H), 7.62 (d, *J* = 7.9 Hz, 1H), 10.11 (s, 1H). MS (ESI): 329.09 (C₁₇H₁₇N₂O₃S, [M+H]⁺). Anal. Calcd for C₁₇H₁₆N₂O₃S: C, 62.18; H, 4.91; N, 8.53; Found: C, 62.27; H, 4.93; N, 8.50.

4.2.23. 2-(5-((4-Methoxybenzyl)thio)-1,3,4-oxadiazol-2-yl)-5-methylphenol (**6w**)

White crystal, yield 65%, mp: 138–139 °C. ¹H NMR (300 MHz, *d*₆-DMSO) δ: 2.31 (s, 3H), 3.73 (s, 3H), 4.51 (s, 2H), 6.83 (d, *J* = 8.0 Hz, 1H), 6.88–6.92 (m, 3H), 7.37–7.41 (m, 2H), 7.62 (d, *J* = 7.9 Hz, 1H), 10.10 (s, 1H). MS (ESI): 329.09 (C₁₇H₁₇N₂O₃S, [M+H]⁺). Anal. Calcd for C₁₇H₁₆N₂O₃S: C, 62.18; H, 4.91; N, 8.53; Found: C, 62.25; H, 4.96; N, 8.50.

4.2.24. 5-Methyl-2-(5-((2-nitrobenzyl)thio)-1,3,4-oxadiazol-2-yl)phenol (**6x**)

White crystal, yield 65%, mp: 187–188 °C. ¹H NMR (300 MHz, *d*₆-DMSO) δ: 2.31 (s, 3H), 4.82 (s, 2H), 6.82 (d, *J* = 7.9 Hz, 1H), 6.88 (s, 1H), 7.61 (t, *J* = 8.9 Hz, 2H), 7.73–7.82 (m, 2H), 8.12 (d, *J* = 8.1 Hz, 1H), 10.10 (s, 1H). MS (ESI): 344.06 (C₁₆H₁₄N₃O₄S, [M+H]⁺). Anal. Calcd for C₁₆H₁₃N₃O₄S: C, 55.07; H, 3.82; N, 12.24; Found: C, 55.04; H, 3.84; N, 12.20.

4.2.25. 5-Methyl-2-(5-((3-nitrobenzyl)thio)-1,3,4-oxadiazol-2-yl)phenol (**6y**)

White crystal, yield 67%, mp: 144–145 °C. ¹H NMR (300 MHz, *d*₆-DMSO) δ: 2.31 (s, 3H), 4.70 (s, 2H), 6.81 (d, *J* = 8.0 Hz, 1H), 6.88 (s, 1H), 7.60 (d, *J* = 8.0 Hz, 1H), 7.65 (t, *J* = 8.0 Hz, 1H), 7.97 (d, *J* = 7.9 Hz, 1H), 8.14–8.17 (m, 1H), 8.40–8.41 (m, 1H), 10.08 (s, 1H). MS (ESI): 344.06 (C₁₆H₁₄N₃O₄S, [M+H]⁺). Anal. Calcd for C₁₆H₁₃N₃O₄S: C, 55.97; H, 3.82; N, 12.24; Found: C, 55.91; H, 3.84; N, 12.20.

4.2.26. 5-Methyl-2-(5-((4-nitrobenzyl)thio)-1,3,4-oxadiazol-2-yl)phenol (**6z**)

White crystal, yield 62%, mp: 162–163 °C. ¹H NMR (300 MHz, *d*₆-DMSO) δ: 2.31 (s, 3H), 4.68 (s, 2H), 6.82 (d, *J* = 8.1 Hz, 1H), 6.88 (s, 1H), 7.60 (d, *J* = 7.9 Hz, 1H), 7.77 (d, *J* = 8.6 Hz, 2H), 8.21 (d, *J* = 8.6 Hz, 2H), 10.10 (s, 1H). MS (ESI): 344.06 (C₁₆H₁₄N₃O₄S, [M+H]⁺). Anal. Calcd for C₁₆H₁₃N₃O₄S: C, 55.97; H, 3.82; N, 12.24; Found: C, 55.99; H, 3.84; N, 12.21.

4.3. Biological assay

4.3.1. Animals

BALB/c mice, 6–8 week-old, were purchased from Experimental Animal Center of Yangzhou University (Yangzhou, China) and were maintained in a controlled environment (12-h light/12-h dark photoperiod, 22 ± 2 °C, 55% ± 5% relative humidity and free access to pellet food and water). All husbandry and experimental contacts made with the mice were maintained at specific pathogen-free conditions. All experimental procedures were carried out strictly according to the guide for the care and use of laboratory animals

(National Research Council of USA, 1996). All efforts were made to minimize animals' suffering and to reduce the number of animals used.

4.3.2. Reagents and materials

T cells were incubated in RPMI 1640 medium supplemented with 10% fetal bovine serum (FBS) (Invitrogen), 100 U/mL of penicillin and 100 µg/mL of streptomycin at 37 °C in a humidified atmosphere containing 5% CO₂. DMSO as a stock solution, was stored at –20 °C and diluted with medium before each experiment. The final DMSO concentration did not exceed 0.1% throughout the study. Other drugs and reagents used in this study were as follows: 3-(4,5-dimethyl-2-thiazolyl)-2,5-diphenyl-2H-tetrazolium bromide (MTT, Sigma Chemical Co., St. Louis, MO); Cyclosporin A (CsA, Sigma Chemical Co., St. Louis, MO); Concanavalin A (ConA, Sigma Chemical Co., St. Louis, MO); Annexin V-FITC/PI Kit (Jingmei Biotech, Nanjing, China).

4.3.3. Cytotoxicity test

Fresh lymph node cells were obtained from BALB/C mice. Cells were cultured in a 96-well plate at a density of 5 × 10⁵ cells per well. Different compounds were added to each well respectively at the concentration of 10 µM. Cells without treated by compounds were used as the control. The incubation was performed in a humidified, 37 °C, 5% CO₂-containing incubator for 24 h. 20 µL of MTT (Sigma, MO; 4 mg/mL in PBS) was added to each well 4 h before the end of the incubation. MTT formazan production was dissolved in 200 µL DMSO replacing the medium at 37 °C for 30 min. The absorbance was read on an ELISA reader (Tecan, Austria) at 570 nm (OD₅₇₀).

4.3.4. Inhibitory activity assay

Fresh lymph node cells were obtained from BALB/C mice. 5 × 10⁵ cells per well were cultured in a 96-well plate at the same conditions to that mentioned above. The cultures were stimulated with 5 µg/mL of concanavalin A (ConA) to induce T cell proliferative responses for 24 h. After that, cells were left untreated or treated with compounds at the concentration of 1 µM for 72 h. Twenty microliters of MTT (Sigma, MO; 4 mg/mL in PBS) was added to each well 4 h before the end of the incubation. After removing the supernatant, 200 µL DMSO was added to dissolve the formazan crystals. The absorbance at 570 nm (OD₅₇₀) was read on an ELISA reader (Tecan, Austria).

Inhibitory activity of each compound was calculated using the following formula:

$$\text{Inhibitory activity} = \frac{[\text{Control}(\text{OD}_{570\text{nm}}) - \text{Compounds}(\text{OD}_{570\text{nm}})]}{\text{Control}(\text{OD}_{570\text{nm}})} \times 100\%$$

Cells untreated with compounds were used as the control.

4.3.5. PI3Ks inhibitory assay

The biological activity of the selected compounds **6c**, **6e**, **6f**, **6l**, **6v** and **6z** was evaluated using an isolated enzyme inhibition assay for PI3Ks.^{36,37} All compounds were first screened at a single concentration of 100 µM, and full IC₅₀s were determined for compounds displaying at least 40% of inhibition at this concentration. The results were summarized in Table 3.

4.3.6. Apoptosis assay

Lymph node cells were incubated in a 24-well plate at a density of 3 × 10⁶ cells per well and stimulated with 5 µg/mL of ConA for 24 h. Then different concentrations of compound **6z** were added to each well. 24 h later, cells were harvested and stained with Annexin V-FITC (fluorescein isothiocyanate) and propidium iodide

(PI). And then samples were analyzed by FACSCalibur flow cytometer (Becton Dickinson, San Jose, CA).

4.4. Experimental protocol of modeling study

The PI3K γ -LXX protein-ligand complex crystal structure (3L54.pdb) was chosen as the template for the modeling study of compounds **6v** and **6z** bound to PI3K γ .³⁸ The crystal structure was obtained from the RCSB Protein Data Bank (<http://www.rcsb.org/pdb/home/home.do>).

The molecular docking procedure was performed by using LigandFit protocol within Discovery Studio 3.1. For ligand preparation, the 3D structures of **6v** and **6z** were generated and minimized using Discovery Studio 3.1. For enzyme preparation, the hydrogen atoms were added, and the water and impurities were removed. The whole PI3K γ enzyme was defined as a receptor and the site sphere was selected based on the ligand binding location of LXX, then the LXX molecule was removed and **6z** or **6v** was placed during the molecular docking procedure. Types of interactions of the docked enzyme with ligand were analyzed after the end of molecular docking.

Acknowledgment

The work was financed by National Natural Science Foundation of China (No. J1103512).

References and notes

- Hackstein, H.; Thomson, A. W. *Nat. Rev. Immunol.* **2004**, *4*, 24.
- Kahan, B. D. *Nat. Rev. Immunol.* **2003**, *3*, 831.
- De Jonghe, S.; Marchand, A.; Gao, L. J.; Calleja, A.; Cuveliers, E.; Sienaert, I.; Herman, J.; Clydesdale, G.; Sefrioui, H.; Lin, Y.; Pfeleiderer, W.; Waer, M.; Herdewijn, P. *Bioorg. Med. Chem. Lett.* **2011**, *21*, 145.
- Wang, Y. R. *Chin. J. New Drugs* **2002**, *11*, 512.
- Wang, X. L.; Tang, F.; Li, H. M. *J. Chin. Phys.* **2002**, *4*, 1291.
- Sheikh-Hamad, D.; Nadkarni, V.; Choi, Y. J.; Truong, L. D.; Wideman, C.; Hodjati, R.; Gabbay, K. H. *J. Am. Soc. Nephrol.* **2001**, *12*, 2732.
- Miller, L. W. *Am. J. Transplant.* **2002**, *2*, 807.
- Smith, J. M.; Nemeth, T. L.; McDonald, R. A. *Pediatr. Clin. North Am.* **2003**, *50*, 1283.
- Cantley, L. C. *Science* **2002**, *296*, 1655.
- Ward, S. G.; Finan, P. *Curr. Opin. Pharmacol.* **2003**, *3*, 426.
- Engelman, J. A.; Luo, J.; Cantley, L. C. *Nat. Rev. Genet.* **2006**, *7*, 606.
- Rommel, C.; Camps, M.; Ji, H. *Nat. Rev. Immunol.* **2007**, *7*, 191.
- Marone, R.; Cmiljanovic, V.; Giese, B.; Wymann, M. P. *Biochim. Biophys. Acta* **2008**, *1784*, 159.
- Fougerat, A.; Gayral, S.; Gourdy, P.; Schambourg, A.; Rückle, T.; Schwarz, M. K.; Rommel, C.; Hirsch, E.; Arnal, J. F.; Salles, J. P.; Perret, B.; Breton-Douillon, M.; Wymann, M. P.; Laffargue, M. *Circulation* **2008**, *117*, 1310.
- Camps, M.; Rückle, T.; Ji, H.; Ardisson, V.; Rintelen, F.; Shaw, J.; Ferrandi, C.; Chabert, C.; Gillieron, C.; Francon, B.; Martin, T.; Gretener, D.; Perrin, D.; Leroy, D.; Vitte, P. A.; Hirsch, E.; Wymann, M. P.; Cirillo, R.; Schwarz, M. K.; Rommel, C. *Nat. Med.* **2005**, *11*, 936.
- Rückle, T.; Schwarz, M. K.; Rommel, C. *Nat. Rev. Drug. Disc.* **2006**, *5*, 903.
- Ferrandi, C.; Ardisson, V.; Ferro, P.; Rückle, T.; Zaratin, P.; Ammannati, E.; Hauben, E.; Rommel, C.; Cirillo, R. *J. Pharmacol. Exp. Ther.* **2007**, *322*, 923.
- Dolman, S. J.; Gosselin, F.; O'Shea, P. D.; Davies, I. W. *J. Org. Chem.* **2006**, *71*, 9548.
- Chen, C. J.; Song, B. A.; Yang, S.; Xu, G. F.; Bhadury, P. S.; Jin, L. H.; Hu, D. Y.; Li, Q. Z.; Liu, F.; Xue, W.; Lu, P.; Chen, Z. *Bioorg. Med. Chem.* **2007**, *15*, 3981.
- Zarghi, A.; Tabatabai, S. A.; Faizi, M.; Ahadian, A.; Navabi, P.; Zanganeh, V.; Shafiee, A. *Bioorg. Med. Chem. Lett.* **2005**, *15*, 15.
- Luo, Y. P.; Yang, G. F. *Bioorg. Med. Chem.* **2007**, *15*, 1716.
- Khan, M. T.; Choudhary, M. I.; Khan, K. M.; Rani, M.; Rahman, A. U. *Bioorg. Med. Chem.* **2005**, *13*, 3385.
- Palmer, J. T.; Hirschbein, B. L.; Cheung, H.; McCarter, J.; Janc, J. W.; Yu, W. Z.; Wesolowski, G. *Bioorg. Med. Chem. Lett.* **2006**, *16*, 2909.
- Manjunatha, K.; Prajwal, L. L.; Fernandes, J.; Kumari, N. S. *Eur. J. Med. Chem.* **2010**, *45*, 5225.
- Kumar, H.; Javed, S. A.; Khan, S. A. *Eur. J. Med. Chem.* **2008**, *43*, 2688.
- Chandra, T.; Garg, N.; Lata, S.; Saxena, K. K. *Eur. J. Med. Chem.* **2010**, *45*, 1772.
- Guimaraes, C. R. W.; Boger, D. L.; Jorgensen, W. L. *J. Am. Chem. Soc.* **2005**, *127*, 17377.
- Frantz, B.; O'Neill, E. A. *Science* **1995**, *267*, 270.
- Wu, K. K. *Circulation* **2000**, *102*, 2022.
- Marra, D. E.; Simoncini, T.; Liao, J. K. *Circulation* **2000**, *102*, 2124.
- Cao, R. H.; Chen, Q.; Hou, X. R.; Chen, H. S.; Guan, H. J.; Ma, Y.; Peng, W. L.; Xu, A. L. *Bioorg. Med. Chem.* **2004**, *12*, 4613.
- Chen, L.; Hainrichson, M.; Bourdetsky, D.; Mor, A.; Yaron, S.; Baasov, T. *Bioorg. Med. Chem.* **2008**, *16*, 8940.
- Racan  , L.; Kralj, M.; Šuman, L.; Stojkovic, R.; Kulenovic, T. V.; Grace, K. Z. *Bioorg. Med. Chem.* **2010**, *1038*, 18.
- Pomel, V.; Klicic, J.; Covini, D.; Church, D. D.; Shaw, J. P.; Roulin, K.; Burgat-Charvillon, F.; Valognes, D.; Camps, M.; Chabert, C.; Gillieron, C.; Francon, B.; Perrin, D.; Leroy, D.; Gretener, D.; Nichols, A.; Vitte, P. A.; Carboni, S.; Rommel, C.; Schwarz, M. K.; Rückle, T. *J. Med. Chem.* **2006**, *49*, 3857.
- Vlahos, C. J.; Matter, W. F.; Hui, K. Y.; Brown, R. F. *J. Biol. Chem.* **1994**, *269*, 5241.
- Kendall, J. D.; Rewcastle, G. W.; Frederick, R.; Mawson, C.; Denny, W. A.; Marshall, E. S.; Baguley, B. C.; Chaussade, C.; Jackson, S. P.; Shepherd, P. R. *Bioorg. Med. Chem.* **2007**, *15*, 7677.
- Chaussade, C.; Rewcastle, G. W.; Kendall, J. D.; Denny, W. A.; Cho, K.; Gronning, L. M.; Chong, M. L.; Anagnostou, S. H.; Jackson, S. P.; Daniele, N.; Shepherd, P. R. *Biochem. J.* **2007**, *404*, 44.
- Knight, S. D.; Adams, N. D.; Burgess, J. L.; Chaudhari, A. M.; Darcy, M. G.; Donatelli, C. A.; Luengo, J. I.; Newlander, K. A.; Parrish, C. A.; Ridgers, L. H.; Sarpong, M. A.; Schmidt, S. J.; Van Aller, G. S.; Carson, J. D.; Diamond, M. A.; Elkins, P. A.; Gardiner, C. M.; Garver, E.; Gilbert, S. A.; Gontarek, R. R.; Jackson, J. R.; Kershner, K. L.; Luo, L.; Raha, K.; Sherk, C. S.; Sung, C.-M.; Sutton, D.; Tummino, P. J.; Wegrzyn, R. J.; Auger, K. R.; Dhanak, D. *ACS Med. Chem. Lett.* **2010**, *1*, 39.
- Pomel, V.; Klicic, J.; Covini, D.; Church, D. D.; Shaw, J. P.; Roulin, K.; Burgat-Charvillon, F.; Valognes, D.; Camps, M.; Chabert, C.; Gillieron, C.; Francon, B.; Perrin, D.; Leroy, D.; Gretener, D.; Nichols, A.; Vitte, P. A.; Carboni, S.; Rommel, C.; Schwarz, M. K.; Rückle, T. *J. Med. Chem.* **2006**, *49*, 3857.
- Chaussade, C.; Rewcastle, G. W.; Kendall, J. D.; Denny, W. A.; Cho, K.; Gronning, L. M.; Chong, M. L.; Anagnostou, S. H.; Jackson, S. P.; Daniele, N.; Shepherd, P. R. *Biochem. J.* **2007**, *404*, 449.